Supporting Information

Regioisomeric mono-pyridine functionalized triarylethene: Small AIEgens with isomeric effect and efficient platform for selective and sensitive detection of Pd^{2+} and Fe^{3+}

Atasi Mukherjee and Manab Chakravarty*

Department of chemistry, Birla Institute of Technology and Sciences-Hyderabad Campus

Hyderbad-500078

Table S1. Absorption and emission maxima, quantum yields (Φ_f in %) of **Np-3Py** and **Np-4Py** in different solvents.

Compound	Solvent	Abs λ_{max} (nm)	Emi λ_{max} (nm)	Φ_f (%)
Np-3Py	1,4-Dioxane	327	414	3.18
	Acetonitrile	327	411	0.69
Np-4Py	1,4-Dioxane	333	414	6.01
	Acetonitrile	333	412	2.32

Table S2: The absorbance and emission wavelength after addition of water in different fractions

Compound	f_w (H_2O/MeCN); (v/v) %	Abs λ_{max} (nm)	Emi λ_{max} (nm)	Compound	Abs λ_{max} (nm)	Emi λ_{max} (nm)
Np-3Py	00	327	411	**Np-4Py**	333	412
	10	327	412		333	419
	20	327	412		333	419

	30	327	413		333	420
	40	327	413		333	422
	50	331	413		335	422
	60	331	414		335	427
	70	335	451		338	438
	80	341	453		344	461
	90	341	455		344	464

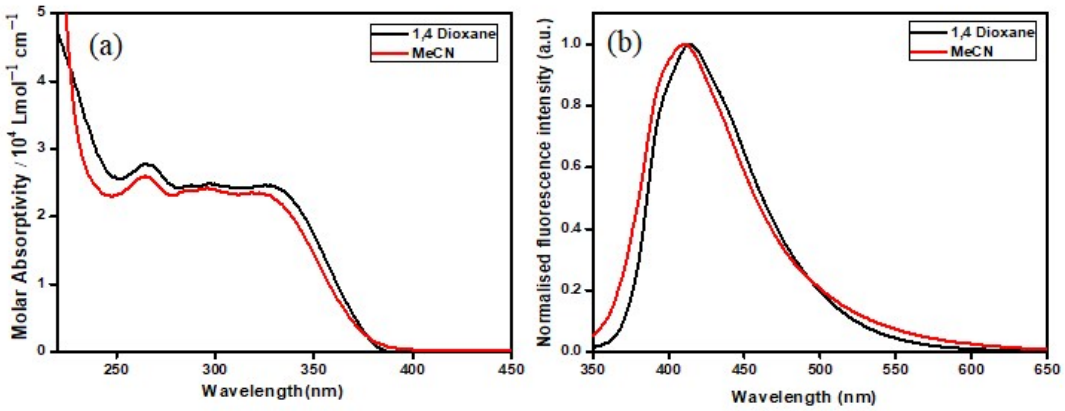

Figure S1. (a) Absorption and (b) emission spectra of **Np-3Py** (10^{-5} M) in different solvents. λ_{ex}= 340 nm.

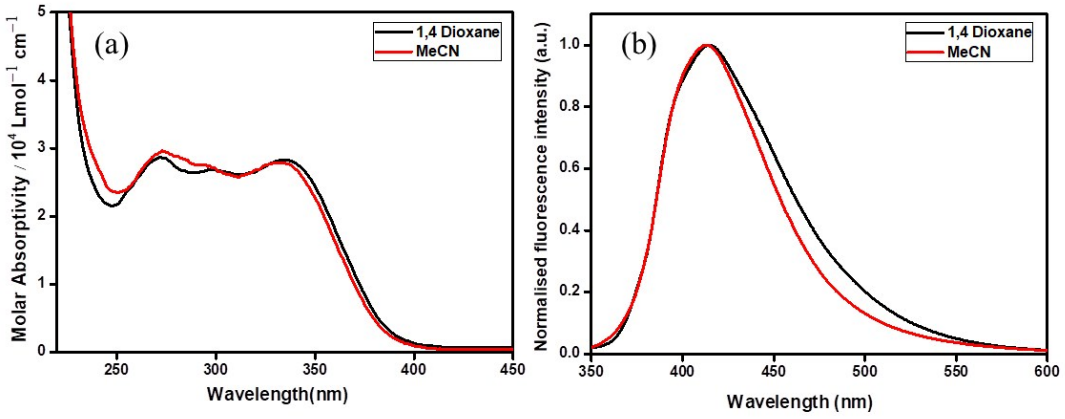

Figure S2. (a) Absorption and (b) emission spectra of **Np-4Py** (10^{-5} M) in different solvents. λ_{ex}= 340 nm.

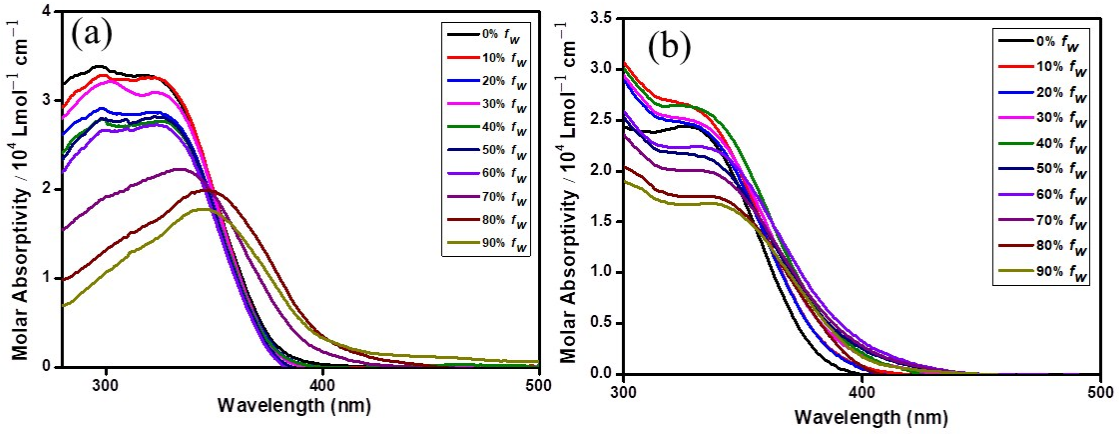

Figure S3. Absorption spectra of (a) **Np-3Py** (10^{-5} M), (b) **Np-4Py** (10^{-5} M) by increasing f_w.

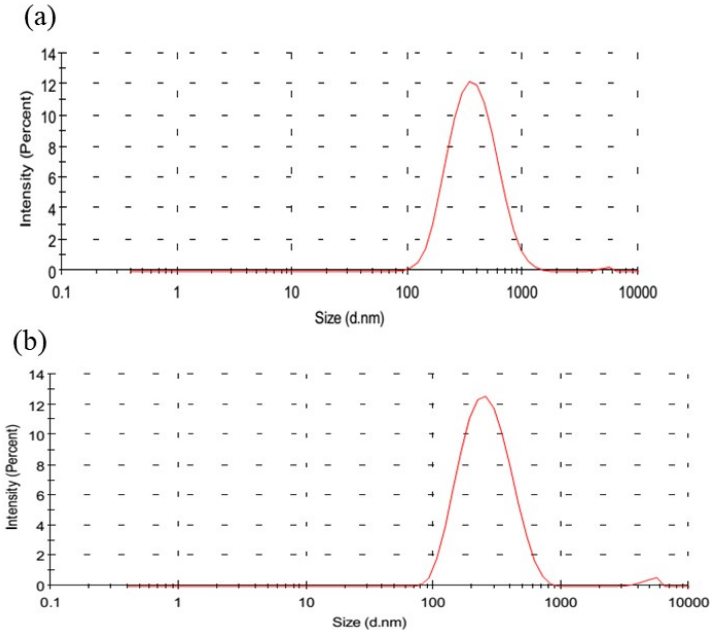

Figure S4. DLS plot of (a) **Np-3Py** and (b) **Np-4Py** to find the average particle size.

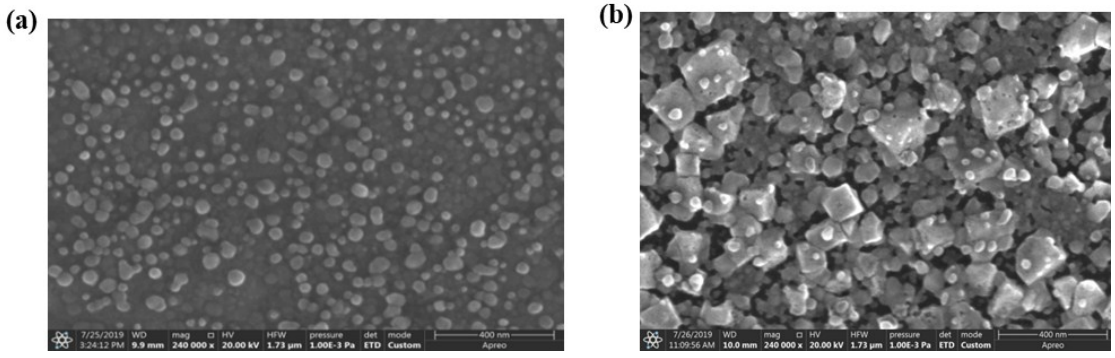

Figure S5. SEM images of (a) molecular (particle size: 46 nm) and (b) aggregate states (particle size: 204 nm) of **Np-3Py**.

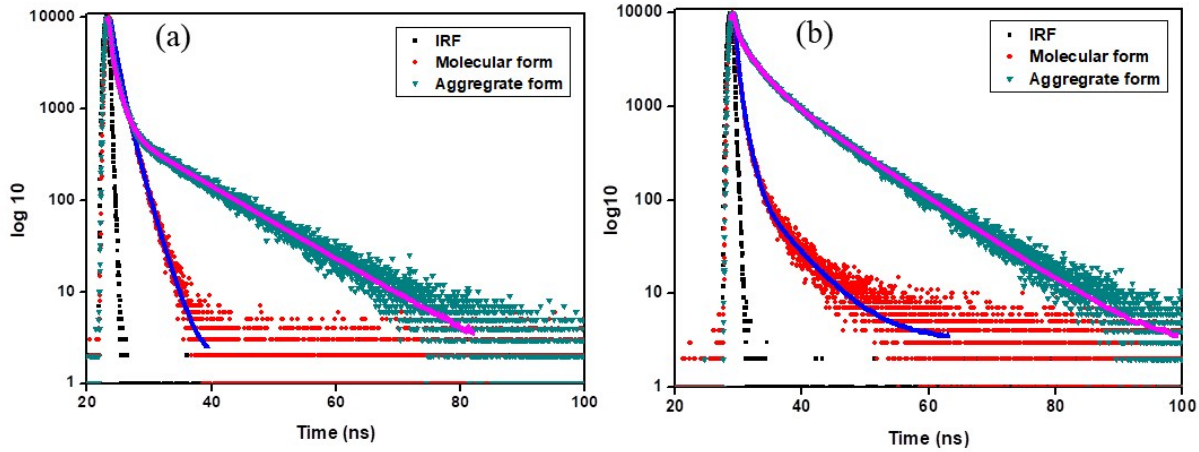

Figure S6. Lifetime decay plots of molecular and aggregate states of (a) **Np-3Py** and (b) **Np-4Py**.

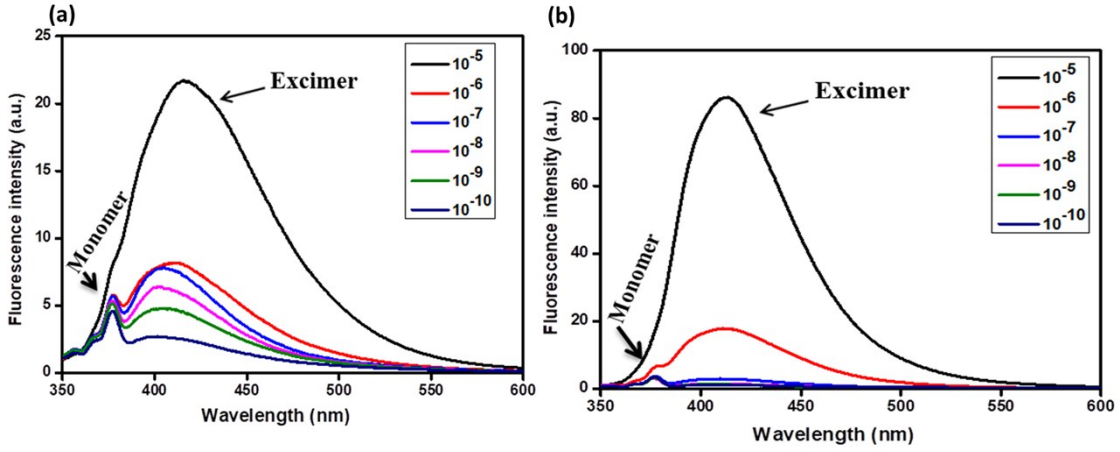

Figure S7. Concentration-dependent emission spectra of (a) **Np-3Py** and (b) **Np-4Py** in acetonitrile. λ_{ex}= 340 nm

Table S3. Life time data for **Np-3Py** and **Np-4Py** in molecular and in aggregate states.

Compound	Form	α_1(%)	α_2(%)	α_3(%)	τ_1(ns)	τ_2(ns)	τ_3(ns)	<τ> (ns)	χ^2
Np-3Py	Molecular	33.45	34.57	31.98	0.14	1.23	10.90	3.96	1.09
	Aggregate	25.32	16.22	58.46	0.13	1.42	11.01	6.70	1.04
Np-4Py	Molecular	58.95	34.19	6.86	0.29	1.05	5.41	4.24	1.18
	Aggregate	13.39	30.55	56.06	0.37	2.86	9.69	6.36	1.23

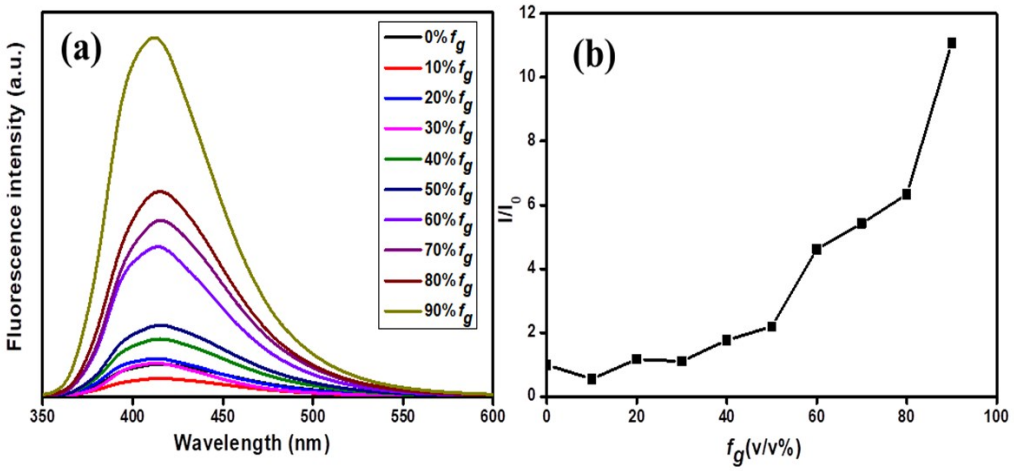

Figure S8A (a) Emission spectra of Np-3Py (10^{-5} M) with di□erent f_g in methanol (b) I/I_0 vs f_g (v/v %) (I_0: initial intensity and I: Intensity after addition of glycerol.) λ_{ex}= 340 nm

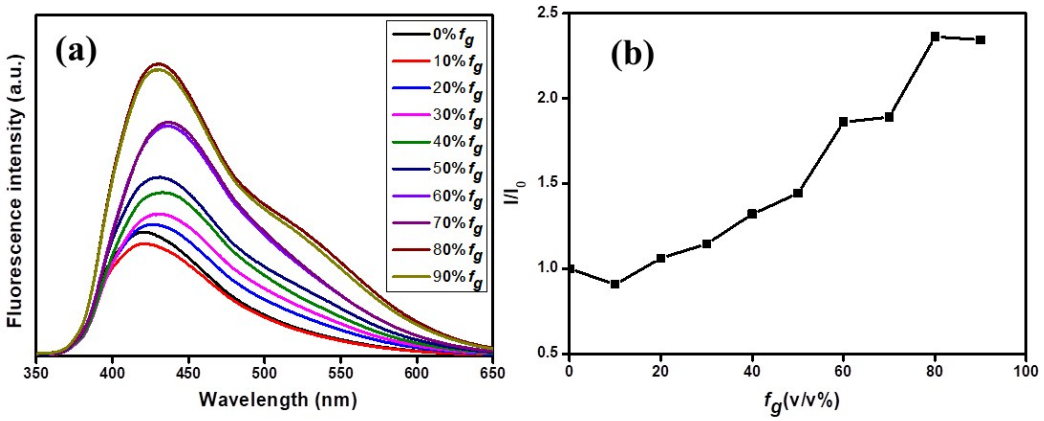

Figure S8B: (a) Emission spectra of **Np-4Py** (10^{-5} M) with di□erent f_g in methanol (b) I/I_0 vs f_g (v/v %) (I_0: initial intensity and I: Intensity after addition of glycerol.) λ_{ex}= 340 nm

Table S4. Crystallographic information for the compounds.

Compound	**Np-3PY**	**Np-4Py**
Emp. Formula	$C_{35}H_{25}N$	$C_{35}H_{25}N$
Formula weight	459.56	459.56
Crystal system	Triclinic	Triclinic
Space group	P -1	P -1
a /Å	7.6570(2)	9.3645(2)
b /Å	10.3364(3)	9.8616(2)
c /Å	15.7530(6)	29.8334(6)
α /°	90.747(3)	91.421(2)
β/°	91.108(3)	95.716(2)

γ/°	106.582(3)	114.431(2)
V /Å^3	1194.49(7)	2489.29(10)
Z	2	2
D_{calc} /g cm^{-3}]	1.278	1.264
μ /mm^{-1}	0.073	0.651
F(000)	484	1001
Data/ restraints/ parameters	6007/0/325	10468/0/649
S	1.012	1.049
R1 [I>2σ(I)]	0.0857	0.0673
wR2 [all data]	0.2320	0.1766
Max./min. residual electron dens. [eÅ^{-3}]	1.208/-0.378	0.334/-0.273

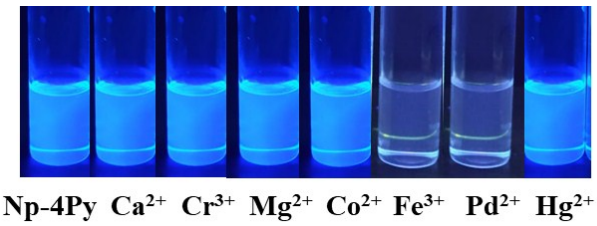

Figure S9. Visual detection of several metal ions by **Np-4Py** (10^{-5} M in 1,4-dioxane), via fluorescence quenching under UV lamp (365 nm). For clarity, other metal ions are excluded, herein.

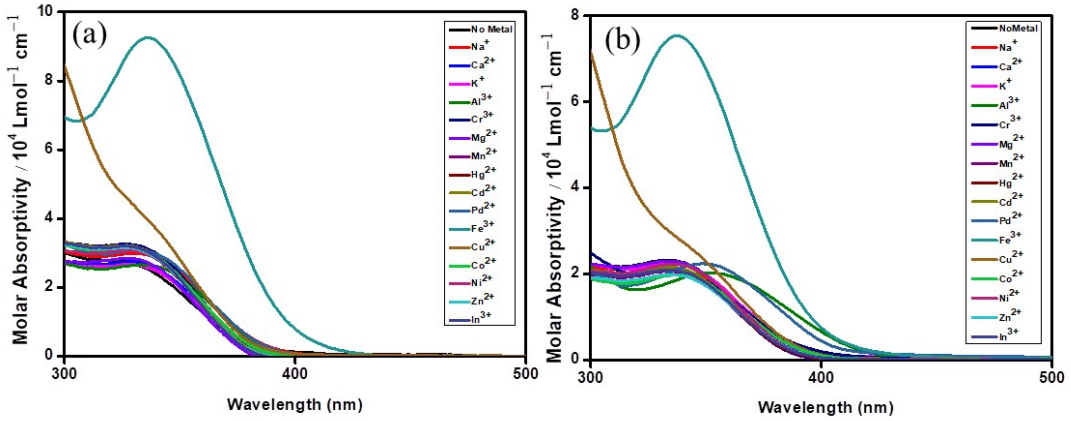

Figure S10. Absorption spectra of (a) **Np-3Py** (10^{-5} M) and (b) **Np-4Py** (10^{-5} M) in 1,4-dioxane in the presence of different metal ions (10^{-4} M).

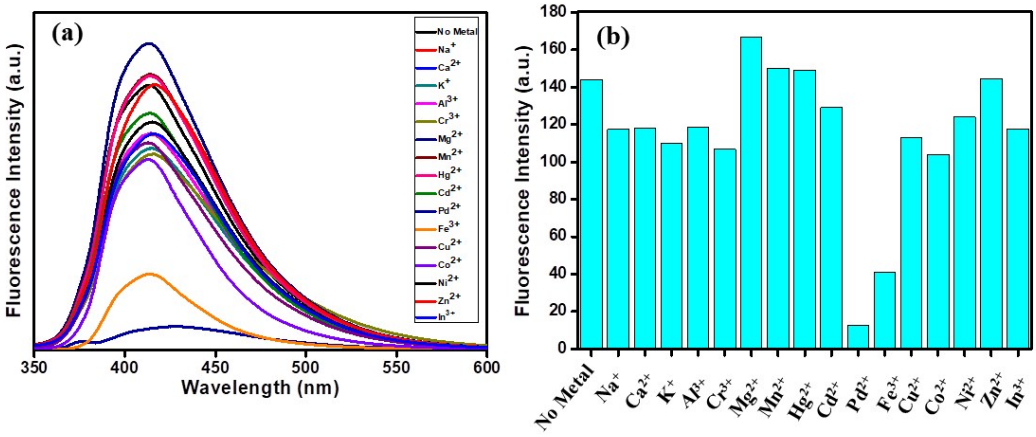

Figure S11. (a) Emission spectra of **Np-4Py** in 1,4-dioxane in the presence of different metal ions. (b) The bar diagram shows the quenching of Pd^{2+} and Fe^{3+} ions. The concentrations of **Np-4Py** and different metal ions are 10^{-5} M and 10^{-4} M, respectively; data error ± 3%. λ_{ex}= 340 nm

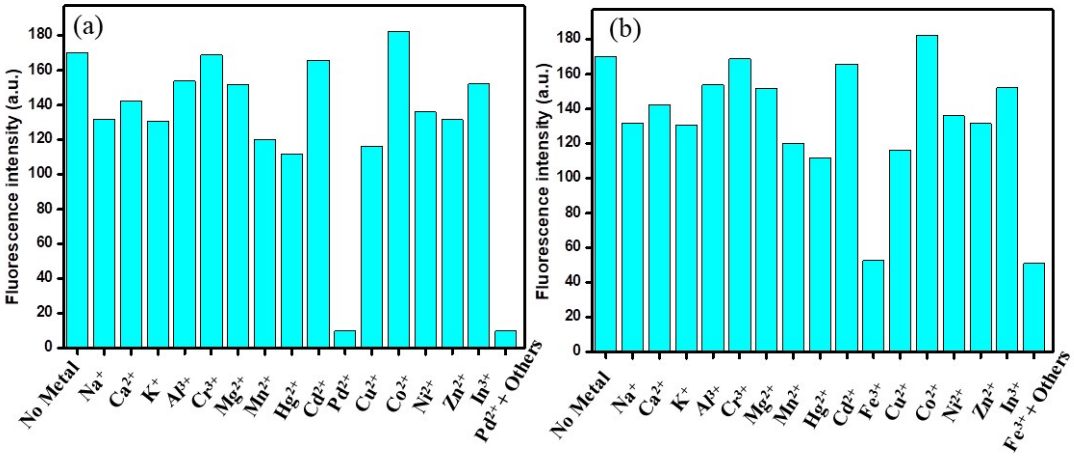

Figure S12. The bar diagrams of **Np-3Py** shows the quenching of (a) Pd^{2+} and (b) Fe^{3+} ions in the presence of all other metal ions (tested herein). The concentrations of **Np-3Py** and different metal ions are 10^{-5} M and 10^{-4} M, respectively; data error ± 3%.

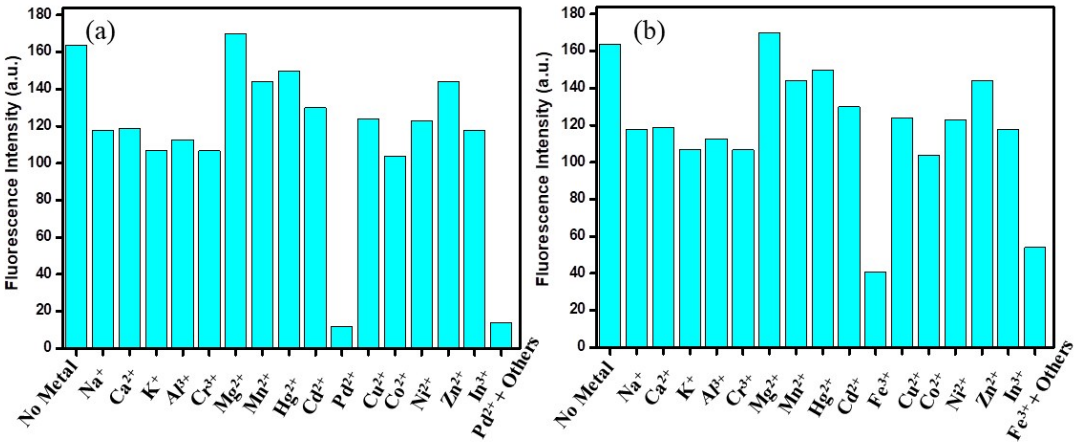

Figure S13. The bar diagrams of **Np-4Py** shows the quenching of (a) Pd^{2+} and (b) Fe^{3+} ions in the presence of all other metal ions (tested herein). The concentrations of **Np-4Py** and different metal ions are 10^{-5} M and 10^{-4} M, respectively; data error ± 3%.

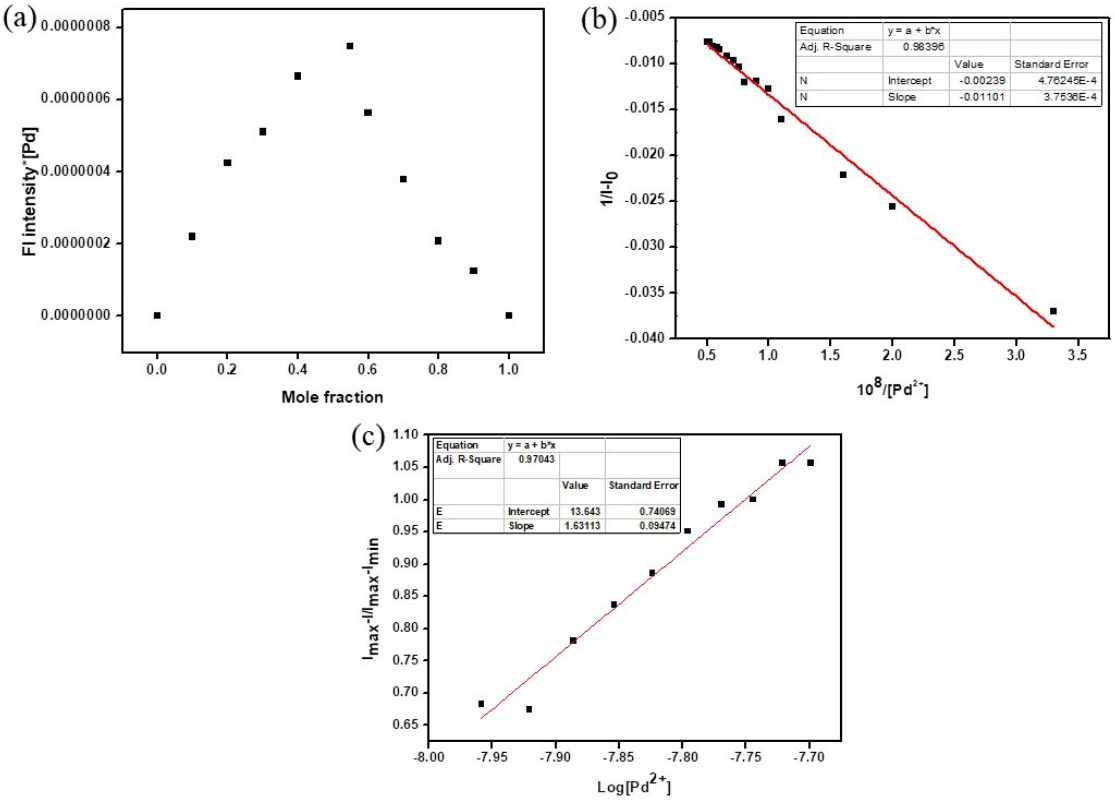

Figure S14. (a) Job's plot, (b) binding constant, (c) detection limit (method 1) of **Np-3Py** for Pd^{2+} (in 1,4 dioxane).

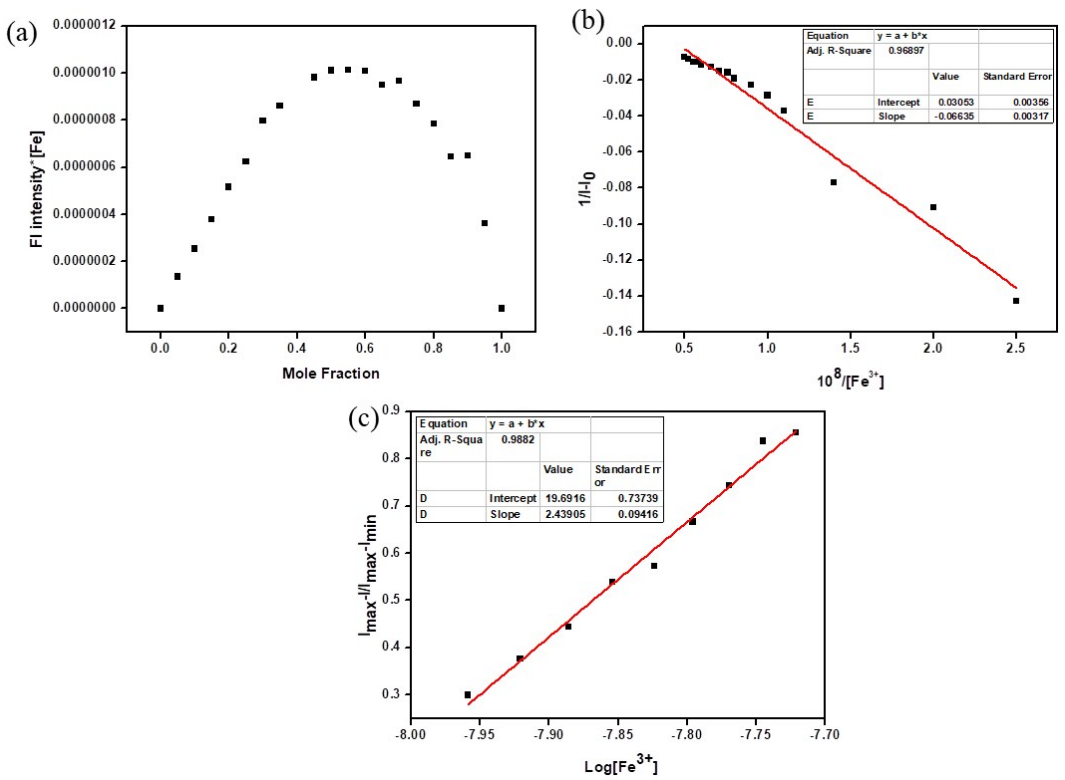

Figure S15. (a) Job's plot, (b) binding constant, (c) detection limit (method 1) of **Np-3Py** for Fe^{3+} (in 1, 4 dioxane).

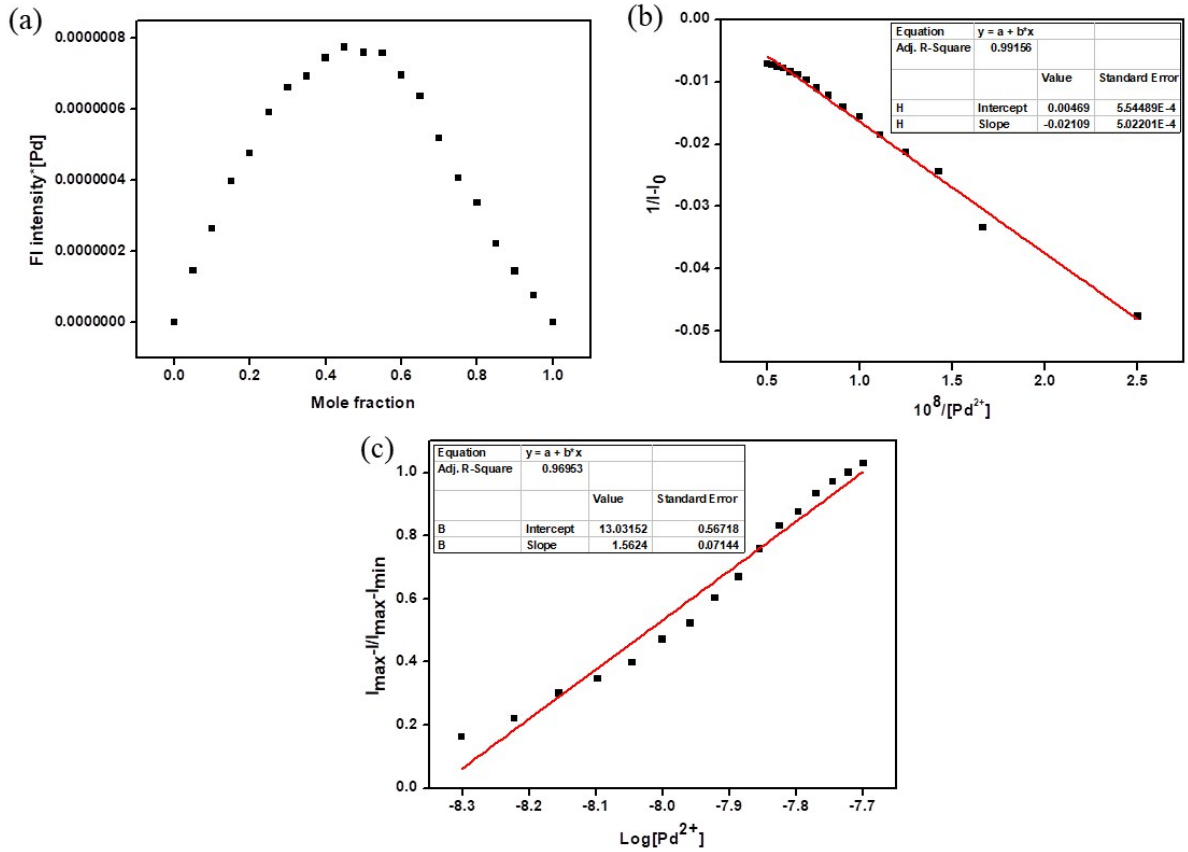

Figure S16. (a) Job's plot, (b) binding constant,(c) detection limit (method 1) of **Np-4Py** for Pd^{2+} (in 1, 4 dioxane).

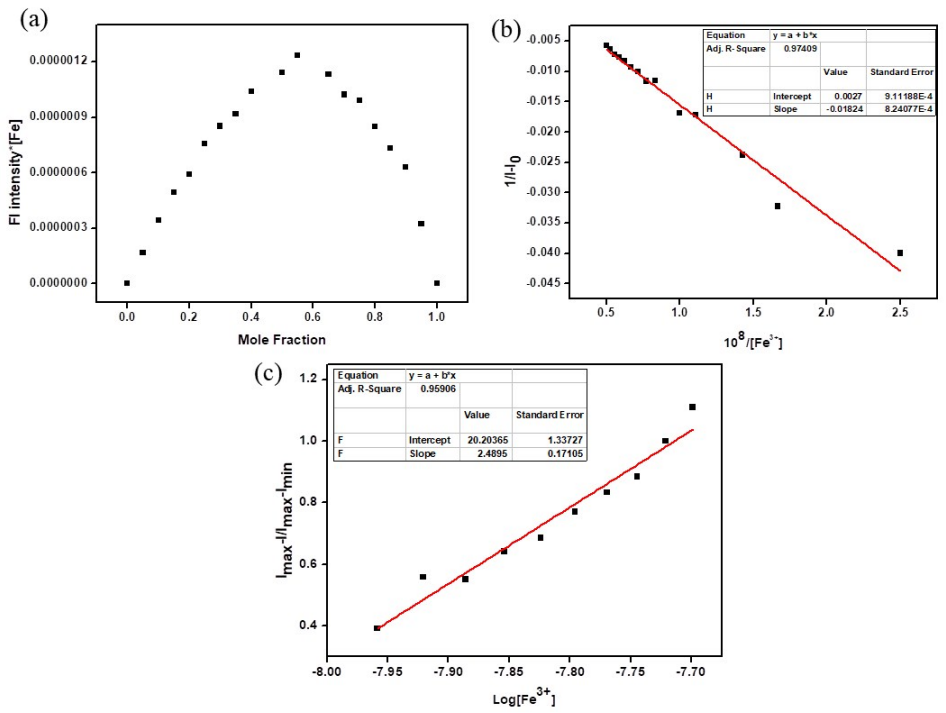

Figure S17. (a) Job's plot,(b) binding constant, (c) detection limit (method 1) of **Np-4Py** for Fe^{3+} (in 1, 4 dioxane).

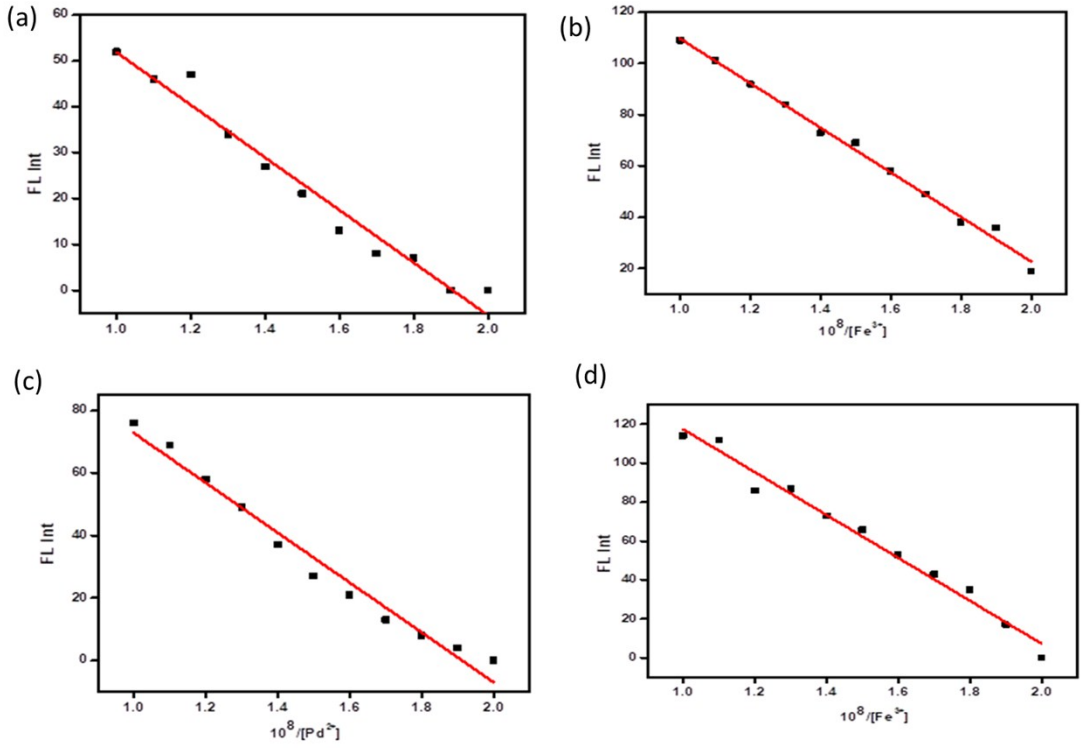

Figure S18: Detection limit (method 2) of **Np-3Py** for (a) Pd^{2+} (b) Fe^{3+}; of **Np-4Py** (c) Pd^{2+} (d) Fe^{3+} in 1, 4 dioxane.

Table S5. Lifetime data for **Np-3Py** and **Np-4Py** with Pd^{2+} and Fe^{3+} ions in 1, 4 dioxane.

Compound	With metal ions	α_1(%)	α_2(%)	α_3(%)	τ_1(ns)	τ_2(ns)	τ_3(ns)	<τ> (ns)	χ^2
Np-3Py	Probe	61.82	20.36	17.82	0.16	1.02	14.97	2.97	1.06
	Fe^{3+}	68.92	15.14	15.94	0.15	1.15	14.87	2.65	1.10
	Pd^{2+}	18.99	79.86	1.15	0.28	0.89	3.09	0.79	1.10
Np-4Py	Probe	35.48	15.17	49.35	0.21	2.44	13.24	6.98	1.19
	Fe^{3+}	34.17	21.81	44.02	0.24	3.25	13.40	6.69	1.19
	Pd^{2+}	36.23	17.26	46.51	0.19	1.37	5.47	2.85	1.11

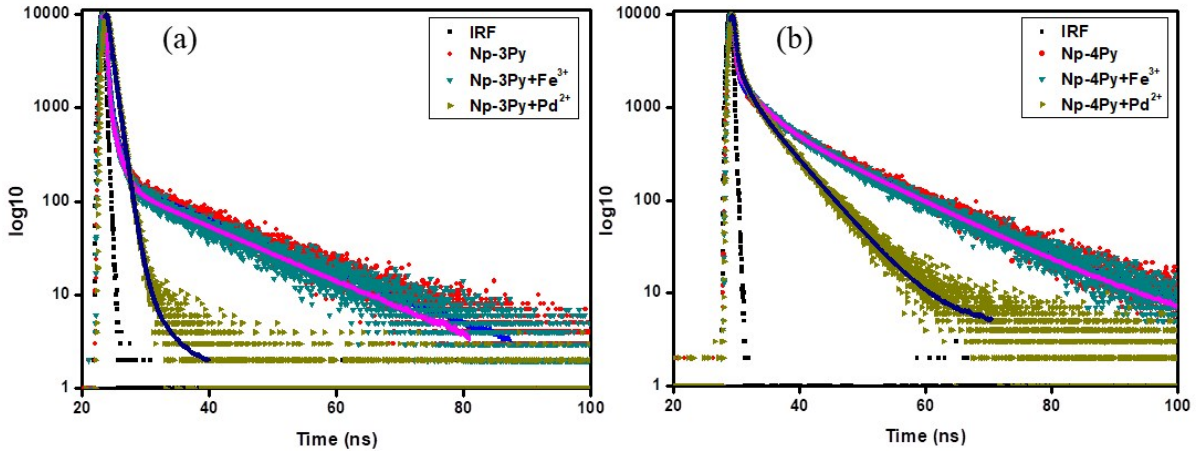

Figure S19. Lifetime decay plots of (a) **Np-3Py** and (b) **Np-4Py** with Pd^{2+} and Fe^{3+} ions in 1, 4 dioxane.

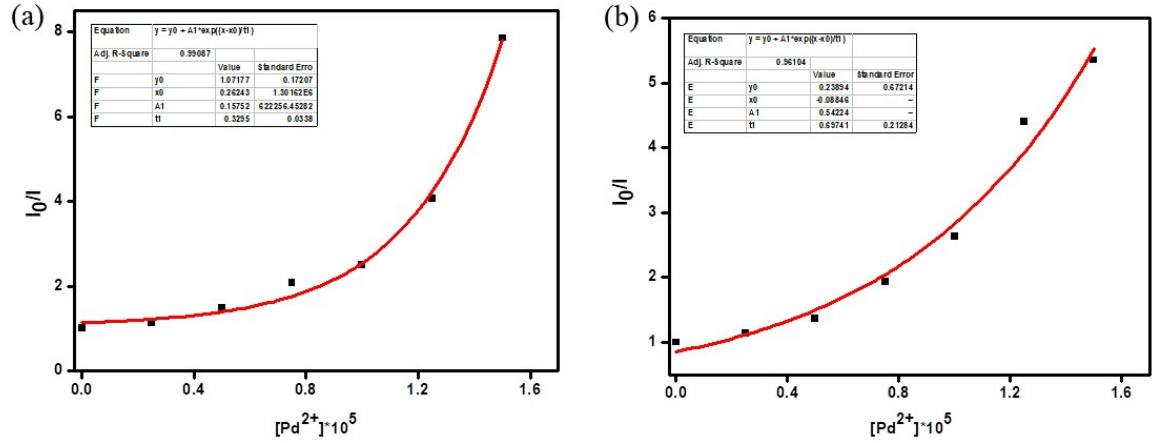

Figure S20. Stern-Volmer Plot of I_0/I vs conc. of Pd^{2+} ion in 1, 4 dioxane for (a) **Np-3Py** and (b) **Np-4Py**.

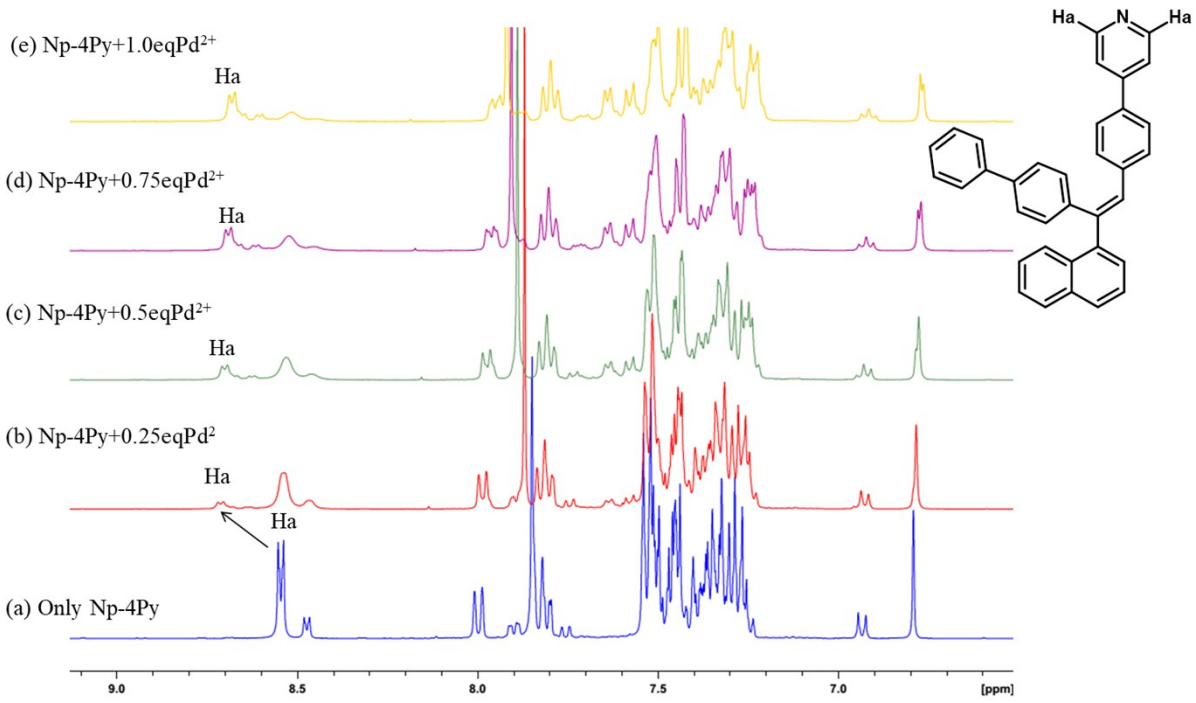

Figure S21. Partial ^{1}H NMR spectra obtained from the titration of compound **Np-4Py** (dr 83:17) with Pd^{2+} in DMSO-d_6.

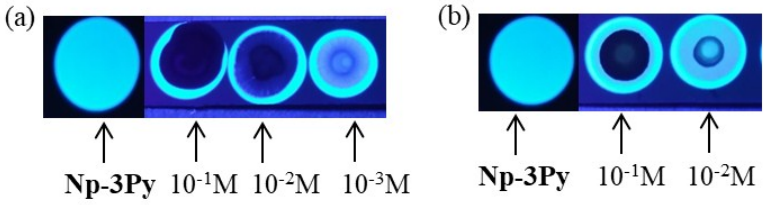

Figure S22. Photographs of **Np-3Py** with (a) Pd^{2+} and (b) Fe^{3+} ions on the TLC plates under UV-lamp (365 nm). TLC plates were made by drop-casting of 10 μM appropriate solution and dried thoroughly.

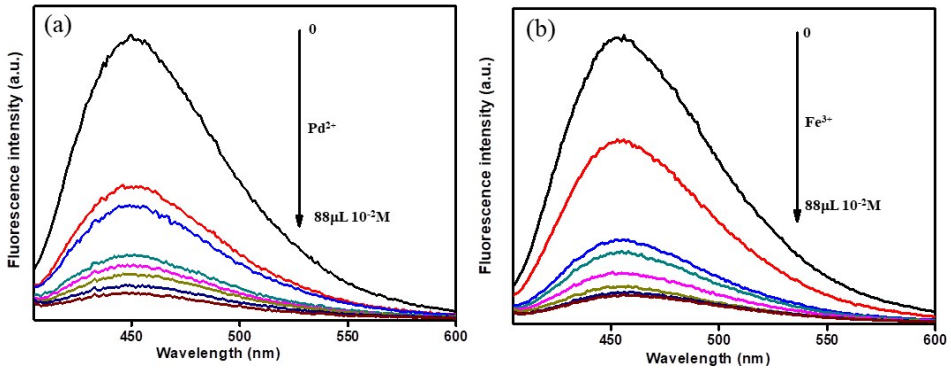

Figure S23. Solid state emission spectrum of **Np-3Py** with (a) Pd^{2+} and (b) Fe^{3+} ions. (**Np-3Py** was mixing with an aqueous solution of Pd^{2+} (10^{-2}/10^{-3} M) and Fe^{3+} (10^{-2} M) ions and dried thoroughly.) λ_{ex}= 340 nm

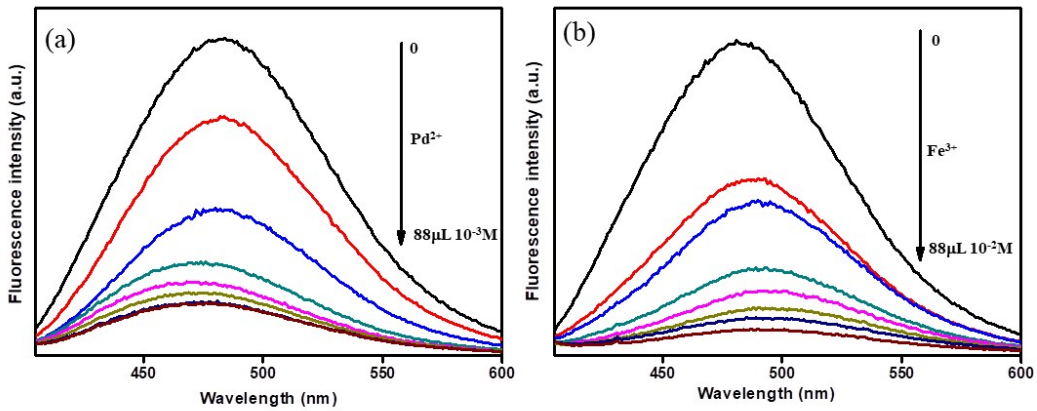

Figure S24. Solid state emission spectrum of **Np-4Py** with (a) Pd^{2+} and (b) Fe^{3+} ions. (**Np-4Py** was mixing with an aqueous solution of Pd^{2+} (10^{-2}/10^{-3} M) and Fe^{3+} (10^{-2} M) ions and dried thoroughly.) λ_{ex}= 340 nm

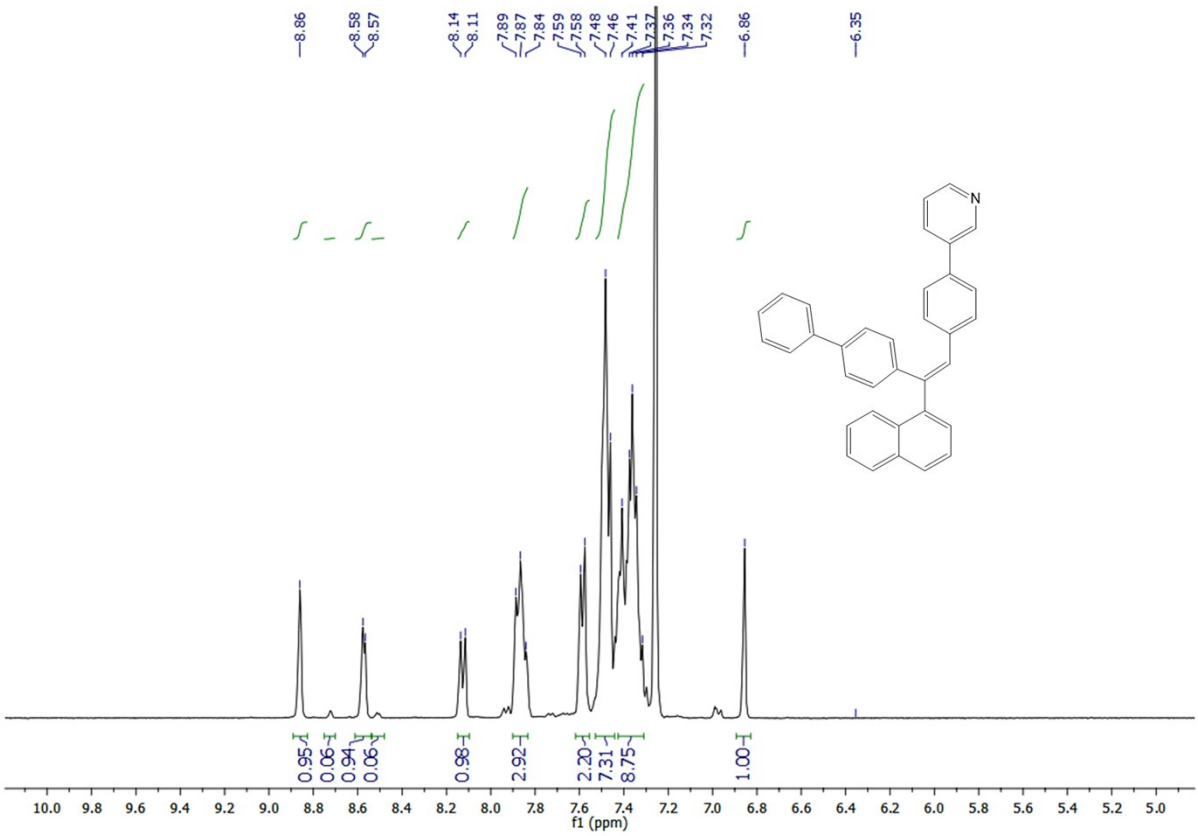

Figure S25. Partial ^{1}H NMR spectra of **Np-3Py** (dr: 94:06).

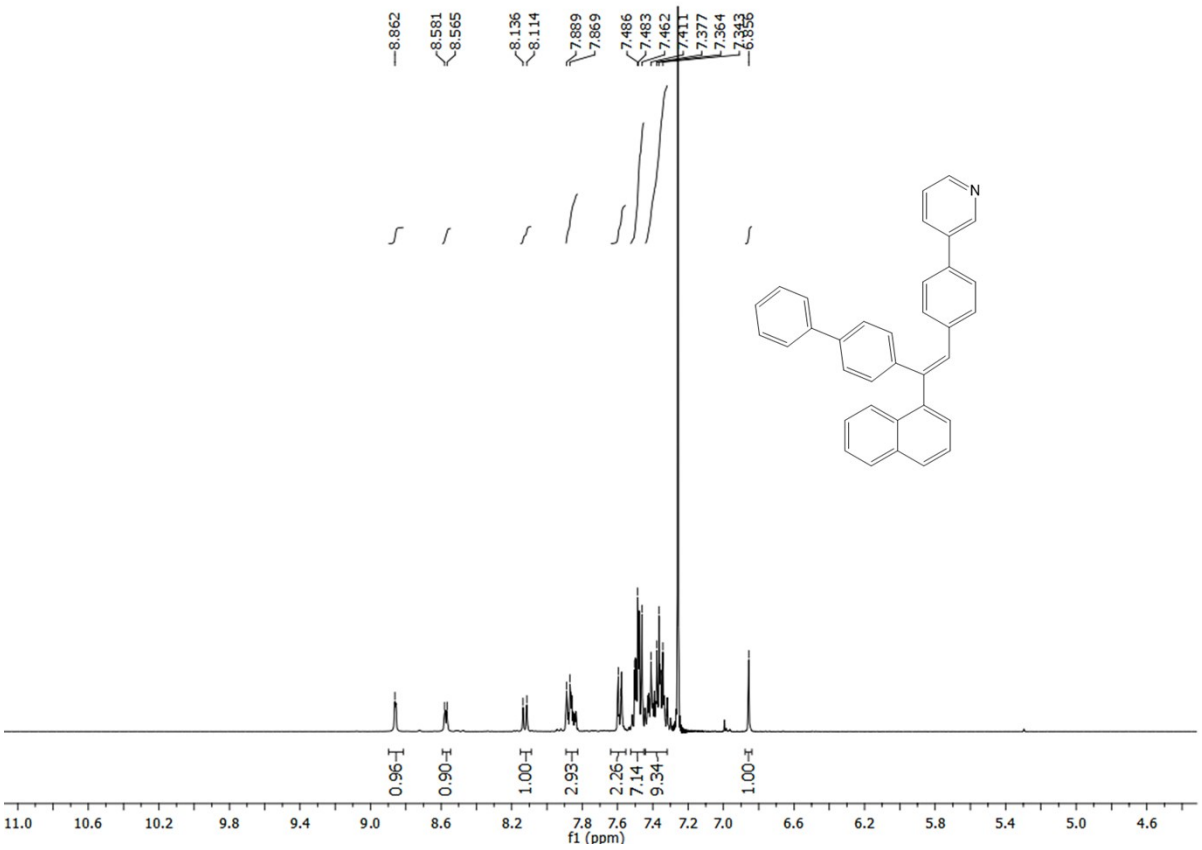

Figure S25a. Partial ^{1}H NMR spectra of **Np-3Py** (crystal)

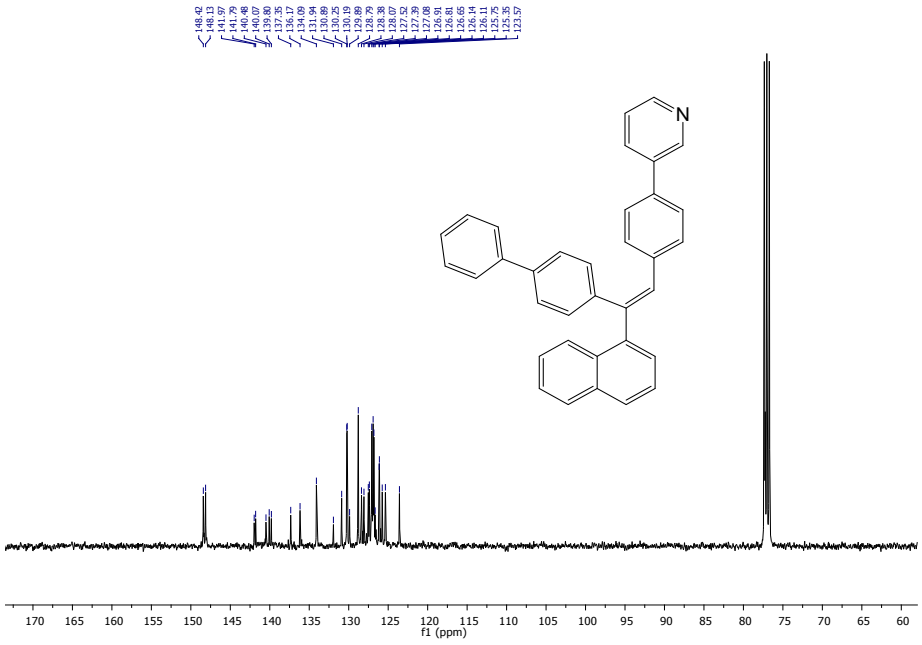

Figure S26. Partial ^{13}C NMR spectra of **Np-3Py** (dr: 94:6).

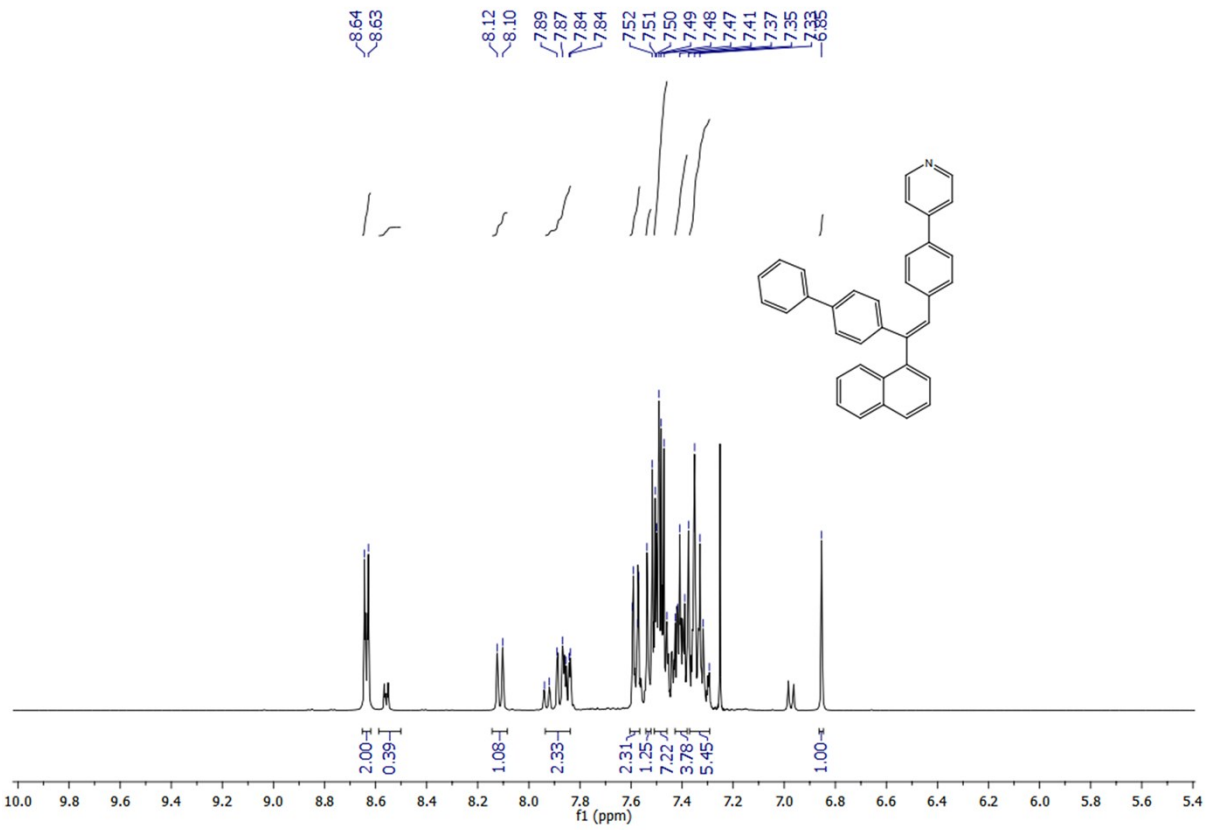

Figure S27. Partial ^{1}H NMR spectra of **Np-4Py** (dr: 83:17).

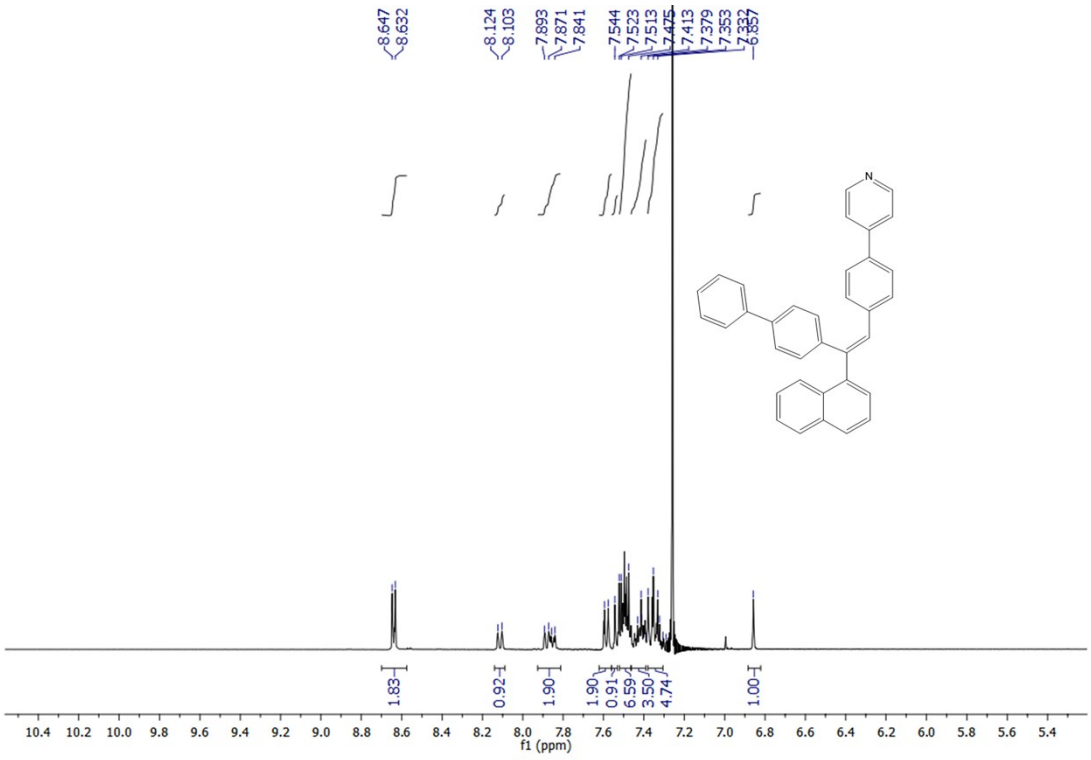

Figure S27a. Partial ^{1}H NMR spectra of **Np-4Py** (Crystal).

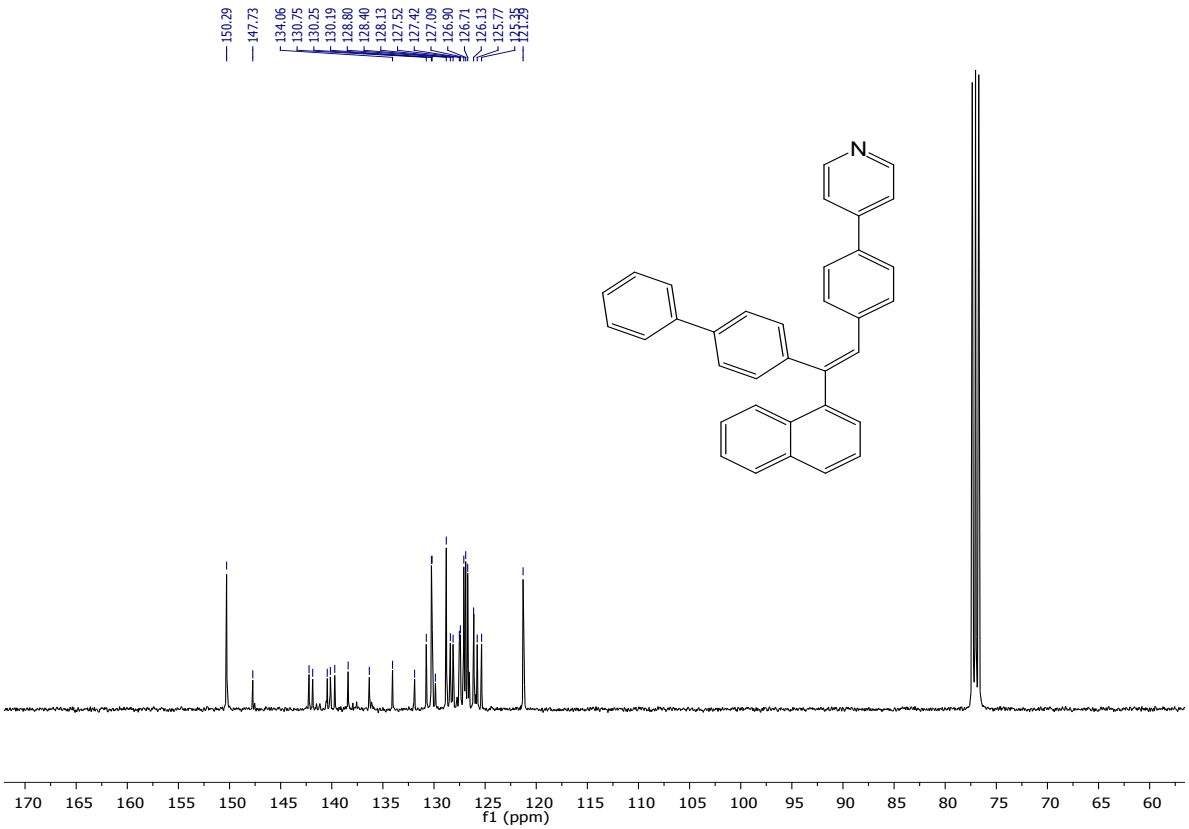

Figure S28. Partial ^{13}C NMR spectra of **Np-4Py** (dr. 83:17).

END